

Sublimation-induced orbital perturbations of extrasolar active asteroids and comets: application to white dwarf systems

Dimitri Veras^{1*}, Siegfried Egg1², Boris T. Gänsicke¹

¹*Department of Physics, University of Warwick, Coventry CV4 7AL, UK*

²*IMCCE Observatoire de Paris, Univ. Lille 1, UPMC, 77 Av. Denfert-Rochereau, 75014 Paris, France*

Accepted 2015 June 23. Received 2015 June 23; in original form 2015 March 26

ABSTRACT

The metal budgets in some white dwarf (WD) atmospheres reveal that volatile-rich circumstellar bodies must both exist in extrasolar systems and survive the giant branch phases of stellar evolution. The resulting behaviour of these active asteroids or comets which orbit WDs is not well-understood, but may be strongly influenced by sublimation due to stellar radiation. Here we develop a model, generally applicable to any extrasolar system with a main sequence or WD star, that traces sublimation-induced orbital element changes in approximately km-sized extrasolar minor planets and comets traveling within hundreds of au. We derive evolution equations on orbital timescales and for arbitrarily steep power-law sublimation dependencies on distance, and place our model in a Solar system context. We also demonstrate the importance of coupling sublimation and general relativity, and the orbital consequences of outgassing in arbitrary directions. We prove that nongravitational accelerations alone cannot result in orbit crossing with the WD disruption radius, but may shrink or expand the orbit by up to several au after a single pericentre passage, potentially affecting subsequent interactions with remnant debris and planets. Our analysis suggests that extant planets must exist in polluted WD systems.

Key words: minor planets, asteroids: general – stars: white dwarfs – methods: numerical – celestial mechanics – planet and satellites: dynamical evolution and stability – protoplanetary discs

1 INTRODUCTION

Water is known to exist in Solar system planets, moons, comets and asteroids. Even after almost 5 Gyr of Solar evolution, active dynamical processes involving water, like the ventilation of plumes on Enceladus (Hansen et al. 2006), persist. Comets still routinely shed their volatile content during close approaches to the Sun. The recent discovery of active asteroids (see Jewitt et al. 2015, for a review) demonstrate that significant amounts of ice can exist in these bodies. But what will happen to the ice and water when the Sun turns off of the main sequence?

The giant branch (GB) phases of evolution are violent, featuring stellar mass loss and intense radiation. In principle, this radiation will evaporate any surface water content of orbiting bodies out to several au, although internal volatiles may be retained (Jura & Xu 2010, 2012). In this paper, we refer to these orbiting bodies as two types: *comets* and *minor*

planets. In the context of exoplanetary systems, we define comets as bodies that formed beyond the snow/frost line, the line at which water and other volatiles froze out during system formation. The volatile content of comets may approach 100 per cent, and represent a complex cocktail of e.g. water ice, carbon dioxide, carbon monoxide, and methane. Alternatively, minor planets formed closer to the star, and hence are less volatile-rich.

Whatever events do occur during the GB phases, we have concrete observational evidence of the final outcome after the stars have become white dwarfs (WDs): atmospheric metal pollution with a high volatile content (Farihi et al. 2013; Raddi et al. 2015). In the case of the WD named GD 61, Farihi et al. (2013) found that the progenitor of the debris in the atmosphere was 26 per cent water by mass; Raddi et al. (2015) later found that the atmosphere of the WD named SDSS J124231.07+522626.6 is enriched with elements that arose from a progenitor that was 38 per cent water by mass.

Between one quarter and one half of all WDs harbour

* E-mail: d.veras@warwick.ac.uk

metal-polluted atmospheres (Zuckerman et al. 2003, 2010; Koester et al. 2014). The dense nature of WDs and the resulting fast sinking times (e.g. Fig. 1 of Wyatt et al. 2014) in their atmospheres indicate that the currently-observed metals do not arise from GB remnants nor internal dredge-up. Further, the spatial distribution and density of interstellar medium clouds prevent the metal pollution from originating there (Aannestad et al. 1993; Friedrich et al. 2004; Jura 2006; Kilic & Redfield 2007; Farihi et al. 2010). Instead, the metal pollution must arise from circumstellar material; bolstering this hypothesis is the presence of orbiting dusty and gaseous discs.

All 37 discs discovered around WDs so far contain dust (Zuckerman & Becklin 1987; Becklin et al. 2005; Kilic et al. 2005; Reach et al. 2005; Farihi et al. 2009; Bergfors et al. 2014; Rocchetto et al. 2015); 7 of them also contain strong gaseous components (Gänsicke et al. 2006, 2007, 2008; Gänsicke 2011; Farihi et al. 2012; Melis et al. 2012; Wilson et al. 2014; Manser et al. 2015; Wilson et al. 2015). These discs exist in exceptionally compact configurations ($\sim 0.6 - 1.2R_{\odot}$, where R_{\odot} is the Solar radius) that are unlike anything which is observed in the Solar system, and are thought to arise from the tidal disruption of minor planets (Graham et al. 1990; Jura 2003; Debes et al. 2012; Bear & Soker 2013; Veras et al. 2014a) and subsequent circularization of the resulting debris (Veras et al. 2015b). The disruption of comets is assumed to provide a smaller contribution to these discs, but is important otherwise for delivering large quantities of hydrogen to WD atmospheres (Veras et al. 2014c; Stone et al. 2015).

The minor planets or comets disrupt by entering the disruption (or Roche) radius – located at a distance of approximately $1R_{\odot}$ – from a relatively great distance of at least several au, and hence contain eccentricities near unity. The semimajor axes of the minor planets or comets must be several au because otherwise they would have been engulfed by the expanding stellar envelope of the GB star. Surviving grains, pebbles, comets, and minor and major planets are affected by a variety of other forces which may perturb these bodies to greater distances (Veras et al. 2015a). Planets are usually too large to be affected by forces other than stellar mass loss (Omarov 1962; Hadjidemetriou 1963; Veras et al. 2011; Adams et al. 2013; Veras et al. 2013a). Minor planets and comets, however, will also be perturbed by the Yarkovsky effect (Veras et al. 2015a), the YORP effect (Veras et al. 2014b), Poynting-Robertson drag and radiation pressure (Bonsor & Wyatt 2010; Veras et al. 2015a), and possibly stellar wind drag (Dong et al. 2010; Veras et al. 2015a), much less any binary stellar companions (Kratter & Perets 2012; Veras & Tout 2012) or surviving planets in the system (Debes & Sigurdsson 2002; Bonsor et al. 2011; Debes et al. 2012; Veras et al. 2013b; Voyatzis et al. 2013; Frewen & Hansen 2014; Mustill et al. 2014; Veras & Gänsicke 2015).

Such complications ensure that minor planets and comets will exist on a wide variety of orbits around WDs, and not necessarily ones which enter the WD’s disruption sphere. So what happens to the volatile-rich minor planets and comets which *miss* the disruption sphere? In this work, we isolate the orbital effects of the sublimation and outgassing of volatiles due to WD radiation, and focus on the minor planets with highly eccentric orbits that fail to reach

the WD disruption radius. Our results are also applicable to a broad variety of comets, as long as their volatile content is not high enough to lead to break up or non-periodic behaviour. We create orbital models which are widely applicable to nearly any extrasolar system assuming that no major planets interfere with the minor planet’s orbit.

In Section 2, we outline our model assumptions for volatile sublimation. Section 3 contains the resulting un-averaged orbital element evolution equations, along with a few applications, demonstrating both the interplay of general relativity and sublimation and the nearly-fixed nature of the orbital pericentre. We then reconsider how this pericentre might change due to outgassing in Section 4, where we also relate the extrasolar and Solar system sublimation models. We discuss the implications in Section 5 and conclude in Section 6. The Appendix contains an extension of our sublimation model that removes the key assumption of a specific power-law exponent.

2 SUBLIMATION MODEL BASICS AND MOTIVATION

Centuries of observations of Solar system comets reveal orbital changes at each apparition. These changes, which can represent shifts in semimajor axis and perihelion of tenths of an au on short timescales (e.g. see Section 5 and Figure 3 of Szutowicz 2000, and Maquet 2015) may have dramatic long-term consequences. Sungrazing comets often are destroyed outright (e.g. Brown et al. 2011), such as C/2012 S1 ISON (Knight & Battams 2014). Orbital alterations are primarily caused by two factors: (1) gravitational interactions due to the architecture of the Solar system, which contains many major and minor planets and moons, and (2) nongravitational forces.

The presence of volatiles ensures that the nongravitational forces from sublimation and outgassing will dominate those from radiation pressure, Poynting-Robertson drag, the Yarkovsky effect and YORP. By *sublimation* we refer to the mass exodus of surface particles which are distributed approximately evenly over large parts of the minor planet or cometary surface. By *outgassing* we refer to localized violent eruptions of material in random directions. This section and Section 3 covers sublimation, and Section 4 covers outgassing.

Minor planets which are strongly affected by sublimation or outgassing are known as “active asteroids” (e.g. Jewitt et al. 2015). Classically, strong outgassing as seen in some comets takes the form of a visibly dramatic tail. Modern observations reveal that the situation is much more complex, sometimes including up to six tails for an individual object (Jewitt et al. 2013).

Consequently, small-body sublimation and outgassing has predominately been investigated observationally in the context of the Solar system and from the perspective of an observer on Earth. Theoretical developments have largely followed suit. Here, however, we consider sublimation from a more general perspective, for application to exoplanetary systems. For WD systems, we have not yet directly detected comets, major planets¹, moons nor any intact minor planets,

¹ The object WD 0806-661 b is by many definitions a bona-

and hence cannot utilise many of the tools developed for or assumptions about the Solar system.

2.1 Physical properties of the minor planet

Denote the mass of the minor planet as M , which contains both a rocky non-volatile component of mass M_c and a volatile component of mass M_v such that

$$M = M_c + M_v. \quad (1)$$

The non-volatile content may be thought of as the minor planet's *core*, although we need not make a priori assumptions about just where the volatiles are located. We consider only minor planets that will remain largely intact, such that they do not fragment or sublimate away a large fraction of their mass. Consequently, the assumption that we do make is that $M_c \gg M_v$, so that $M \approx M_c$ remains constant over the number of pericentre passages needed for all of M_v to sublimate away. This assumption is robust for minor planets and many types of comets. Alternately, for some comets, M_v/M may approach unity. In this case, the dynamical evolution can change in more drastic ways than we report here.

The rotation state of the minor planet will crucially determine where outgassing will occur, with consequences for the minor planet's orbital evolution. Chesley & Yeomans (2005) have shown that outgassing via jets can be modeled in an average sense, if the rotation of the object is well defined. Their model suggests that outgassing is predominately happening on the starlit hemisphere on slow rotators with low thermal inertia. Yet, outgassing itself will likely change the rotation state of the minor planet (Mottola et al. 2014), thereby randomizing the perturbations and emphasizing the stochasticity of the process of outgassing. Stochastic variations intrinsically contain time-dependent variations in direction and magnitude, as would occur in a tumbling minor planet. The actual accelerations will be probabilistically distributed (e.g. Pierret 2014).

Treating potentially complex rotation is beyond the scope of the present work and beyond the scope of our knowledge of minor planets in extrasolar systems. Instead, we consider outgassing from a general perspective in Section 4, rather than assuming outgassing occurs only on the starlit hemisphere, as in Festou et al. (1993).

2.2 Orbital change of the minor planet

Many forces contribute to the orbital motion of the minor planet, including those due to radiation, sublimation and outgassing. Further, minor planets with orbital pericentres close to the WD might be significantly affected by general relativity (GR). If the minor planet has an orbital period similar to those of exo-Oort cloud comets, then near apocentre both Galactic tides and stellar flybys can cause significant perturbations.

Strictly, when a body (like a minor planet) loses mass

the planet orbiting a WD at a distance of about 2500 au (Luhman et al. 2011). Further, an increasingly strong case is being made for a pair of purported planets which orbit a WD - M star binary (Marsh et al. 2014).

anisotropically, its orbit is perturbed by both linear momentum recoil and mass loss. Although fully described analytically (Veras et al. 2013b), the equations of motion due solely to mass loss can be ignored here because $M \ll M_{\text{WD}}$, where M_{WD} is the mass of the WD. The overall change in mass of the system due to sublimation plus outgassing is negligible. The primary perturbations on orbits due to sublimation and outgassing is linear momentum recoil.

Whipple (1950) used conservation of momentum to show that the nongravitational acceleration on a minor planet (\vec{J}_{NG}) is related to its ejecta through

$$M\vec{J}_{\text{NG}} = -Dm_s\vec{v}_g, \quad (2)$$

where m_s is the mass of one molecule of the molecular species that is sublimating, \vec{v}_g is the mean ejection velocity of that species, and D is the number of molecules of that species sublimating per time. For our numerical computations, we will assume the sublimating species is water ice (H_2O), and hence will adopt $m_s = 2.99 \times 10^{-26}$ kg. We assume that most of the sublimation occurs on the starlit hemisphere because the minor planet's tiny thermal inertia will ensure a near-zero thermal wave lag angle (Groussin et al. 2013). Consequently, the complex physics which relates thermal balance, rotation, sublimation and outgassing is simplified here through the values of D and \vec{v}_g .

The equation of motion for the minor planet is

$$\ddot{\vec{r}} = -\frac{G(M_{\text{WD}} + M_c)\vec{r}}{r^3} + \ddot{\vec{r}}_{\text{sub}} + \ddot{\vec{r}}_{\text{extra}}, \quad (3)$$

where

$$\ddot{\vec{r}}_{\text{sub}} = \Theta(M_v)\vec{J}_{\text{NG}}, \quad (4)$$

\vec{r} is the distance between the minor planet and the WD, $\ddot{\vec{r}}_{\text{sub}}$ is the acceleration due to sublimation, $\ddot{\vec{r}}_{\text{extra}}$ is the acceleration due to other forces, and Θ is the Heaviside step function such that $\Theta(M_v) = 1$ when $M_v > 0$, and zero otherwise. Other forces which must be included in $\ddot{\vec{r}}_{\text{extra}}$ depend on the system being studied. These additive terms from other forces have been used or applied in previous investigations: mass loss (Omarov 1962; Hadjidemetriou 1963; Veras et al. 2013a), the Yarkovsky effect (Veras et al. 2015a), the YORP effect (Veras et al. 2014b), Galactic tides (Heisler & Tremaine 1986; Rickman & Froeschlé 1987; Fouchard et al. 2006; Veras & Evans 2013b) and stellar flybys in the Galactic field (Fregeau et al. 2004; Zakamska & Tremaine 2004; Veras & Moekel 2012).

One effect which might strongly influence the orbit of any minor planet or comet with a pericentre close to the star is GR. Solar system studies have indicated the importance of GR in calculations of cometary orbital solutions (e.g. Yeomans et al. 1996; Maquet et al. 2012). Consequently, we do incorporate GR into our formalism. We do not consider the other effects mentioned above any further, and hence set $\ddot{\vec{r}}_{\text{extra}} = \ddot{\vec{r}}_{\text{GR}}$. This assumption is reasonable because large minor planets with low thermal inertia are not strongly affected by Yarkovsky forces. Similarly, sublimation and outgassing dominate the evolution of minor planet spin as long as volatiles are present.

We use the complete expression for the IPN (leading

post-Newtonian) term of GR in the limit of a zero-mass minor planet (equation 3.190 of Beutler 2005)

$$\ddot{\vec{r}}_{\text{GR}} = \frac{GM_{\text{WD}}}{c^2 r^3} \left[\left(\frac{4GM_{\text{WD}}}{r} - v^2 \right) \vec{r} + 4(\vec{v} \cdot \vec{r}) \vec{v} \right] \quad (5)$$

where \vec{v} is the velocity of the minor planet with respect to the star and c is the speed of light.

Now consider equations (2)-(4) in greater depth. In order to develop physical intuition for how the 2-body orbit changes due to linear momentum recoil, we insert equation (4) into equation (3) and reexpress equation (3) in terms of orbital elements. Doing so requires us to express \vec{J}_{NG} in terms of positions and velocities. In general, $D \propto r^{-2}$ (Sosa & Fernández 2009), as the gas production rate peaks at the pericentre. More complex expressions (e.g. Korsun et al. 2014) are Solar system-specific, and are dependent on observables. Also, $\vec{v}_{\text{g}} \propto r^{-1/4}$ (equation 28 of Whipple 1950). We note that this velocity dependence is different from the $r^{-1/2}$ dependence predicted by equation 8 of (Korsun et al. 2010) because the latter is the terminal velocity of the gas, rather than the velocity at the area of the ejection. Assuming that sublimation occurs only on the starlit side, we find $\vec{v}_{\text{g}}/v_{\text{g}} = \vec{r}/r$.

These dependencies yield:

$$\ddot{\vec{r}}_{\text{sub}} = -\Theta(M_{\text{v}}) \frac{D_0 v_{\text{g}0} m_{\text{s}}}{M_{\text{c}}} \left(\frac{r_0}{r} \right)^{\frac{3}{4}} \frac{\vec{r}}{r} \quad (6)$$

where $D = (r_0/r)^2 D_0$ and $\vec{v}_{\text{g}} = v_{\text{g}0} (r_0/r)^{\frac{1}{4}} (\vec{r}/r)$. Although these power-law dependencies are physically-motivated, we realize that other dependencies may be used based on Solar system observations (e.g. Sanzovo et al. 2001). In order to take into account other possibilities, we generalise equation (6) in the Appendix. There we show (in Table A1) our qualitative results hold for steeper power-law dependencies.

We cannot assume that the composition and outgassing properties of extrasolar minor planets are similar to Solar system minor planets because their formation channels may be different and because WDs and the Sun have different power spectra. Nevertheless, we can look towards the Solar system for rough guidance. In the Solar system, representative D_0 values for sublimation are a few orders of magnitude less than the observed outgassing-based values of $D_0 \sim 10^{28} - 10^{31}$ molecules per second (Table 3 of A'Hearn et al. 1995 and Fig. 3 of Sosa & Fernández 2011). The ejection speeds $|\vec{v}_{\text{g}}|$ from the surface are unknown, but the terminal escape speed of the gas is thought to be on the order of cm/s - tens of m/s (Korsun et al. 2010). If r_0 is taken to be at the pericentre of the orbit, then equation (6) effectively models the diminution of the escaping molecules as the minor planet flies away from the WD. This sublimation model is adequate for our purposes.

Real outgassing naturally does not occur in such a well-behaved radially symmetric manner; nonzero tangential components may be significant (e.g. Table 1 of Marsden et al. 1973, Table 2 of Królikowska 2004, and Table 4 of Szutowicz & Rickman 2006). Therefore, the initial conditions for exosystems with minor planets and comets are largely unconstrained by observationally-motivated considerations. Consequently, in Section 4 we consider outgassing from a general analytical perspective that strengthens our

main conclusion without forcing us to resort to specific parameter choices.

Also, for notational ease, we will henceforth drop the $\Theta(M_{\text{v}})$ term in all subsequent equations. Nevertheless, we must determine over what timescale M_{v} is depleted. The volatile budget decreases according to

$$\begin{aligned} M_{\text{v}} &= M_{\text{v}}(0) - \int_0^t m_{\text{s}} D_0 \left(\frac{r_0}{r} \right)^2 dt \\ &\approx M_{\text{v}}(0) - \frac{m_{\text{s}} D_0 r_0^2}{n a^2 \sqrt{1-e^2}} (f - f_0) \end{aligned} \quad (7)$$

$$\begin{aligned} &\approx M_{\text{v}}(0) - 8.6 \times 10^7 \text{kg} \times N \left(\frac{\sqrt{1-0.999^2}}{\sqrt{1-e^2}} \right) \\ &\times \left(\frac{a}{10 \text{au}} \right)^{-1/2} \left(\frac{r_0}{10^{-2} \text{au}} \right)^2 \left(\frac{M}{0.6 M_{\odot}} \right)^{-1/2} \\ &\times \left(\frac{m_{\text{s}}}{2.99 \times 10^{-26} \text{kg}} \right) \left(\frac{D_0}{10^{29} \text{mol/s}} \right) \end{aligned} \quad (8)$$

where N is the approximate number of orbits, n is the mean motion, a is the semimajor axis, e is the eccentricity and f is the true anomaly. The number of orbits over which the entire volatile budget would be depleted is

$$N_{\text{max}} \approx \frac{M_{\text{v}}(0) n_0 a_0^2 \sqrt{1-e_0^2}}{2\pi m_{\text{s}} D_0 r_0^2}. \quad (9)$$

Equation (9) is useful for determining simulation durations, and how much of the body's mass has been lost when the body's orbit begins to undergo major changes. However, that estimate becomes progressively worse as the semimajor axis undergoes drastic variations.

Having obtained an observationally-motivated functional form for sublimation (equation 6), we can now derive the equations of motion in orbital elements to understand how sublimation changes the orbit.

3 UNAVERAGED EQUATIONS OF MOTION FOR SUBLIMATION

As a first step, we consider the equations of motion with as few assumptions as possible. In the subsequent analysis, the following auxiliary set of variables will be useful:

$$C_1 \equiv e \cos \omega + \cos(f + \omega), \quad (10)$$

$$C_2 \equiv e \sin \omega + \sin(f + \omega), \quad (11)$$

$$C_5 \equiv (3 + 4e \cos f + \cos 2f) \sin \omega + 2(e + \cos f) \cos \omega \sin f, \quad (12)$$

$$C_6 \equiv (3 + 4e \cos f + \cos 2f) \cos \omega - 2(e + \cos f) \sin \omega \sin f, \quad (13)$$

$$C_7 \equiv (3 + 2e \cos f - \cos 2f) \cos \omega + \sin \omega \sin 2f, \quad (14)$$

$$C_8 \equiv (3 - \cos 2f) \sin \omega - 2(e + \cos f) \cos \omega \sin f, \quad (15)$$

$$C_9 \equiv (3 + 2e \cos f - \cos 2f) \sin \omega - \cos \omega \sin 2f. \quad (16)$$

This nomenclature was chosen to maintain consistency with previous studies (Veras & Evans 2013a,b; Veras et al. 2013a, 2014d; Veras 2014a) and highlight the naturally-occurring

quantities in many formulations of the perturbed two-body problem, including those with sublimation.

3.1 General orbital evolution equations

In order to obtain the unaveraged equations of motion in orbital elements, we employ the procedure suggested in Veras et al. (2011) and embellished in Veras & Evans (2013a), based on perturbative analyses from Efroimsky (2005) and Gurfil (2007). We find

$$\left(\frac{da}{dt}\right)_{\text{sub}} = \frac{2D_0v_{g0}m_s r_0^{9/4} (1+e \cos f)^{9/4}}{M_c n a^{9/4} (1-e^2)^{11/4}} \times \left[C_1 (\cos i \cos \Omega - \cos i \sin \Omega + \sin i) - C_2 (\cos \Omega + \sin \Omega) \right], \quad (17)$$

$$\left(\frac{de}{dt}\right)_{\text{sub}} = \frac{D_0v_{g0}m_s r_0^{9/4} (1+e \cos f)^{5/4}}{2M_c n a^{13/4} (1-e^2)^{7/4}} \times \left[C_6 (\cos i \cos \Omega - \cos i \sin \Omega + \sin i) - C_5 (\cos \Omega + \sin \Omega) \right], \quad (18)$$

$$\left(\frac{di}{dt}\right)_{\text{sub}} = \frac{D_0v_{g0}m_s r_0^{9/4} (1+e \cos f)^{5/4} \cos(f+\omega)}{M_c n a^{13/4} (1-e^2)^{7/4}} \times \sin i (\sin \Omega - \cos \Omega + \cot i), \quad (19)$$

$$\left(\frac{d\Omega}{dt}\right)_{\text{sub}} = \frac{D_0v_{g0}m_s r_0^{9/4} (1+e \cos f)^{5/4} \sin(f+\omega)}{M_c n a^{13/4} (1-e^2)^{7/4}} \times (\sin \Omega - \cos \Omega + \cot i), \quad (20)$$

$$\left(\frac{d\omega}{dt}\right)_{\text{sub}} = -\frac{D_0v_{g0}m_s r_0^{9/4} (1+e \cos f)^{5/4}}{2M_c n a^{13/4} e (1-e^2)^{7/4}} \times \left[C_8 (\cos i \cos \Omega - \cos i \sin \Omega) + C_9 \sin i + C_7 (\cos \Omega + \sin \Omega) + 2e \sin(f+\omega) \cos i \cot i \right], \quad (21)$$

$$\left(\frac{dq}{dt}\right)_{\text{sub}} = \frac{D_0v_{g0}m_s r_0^{9/4} (1+e \cos f)^{5/4}}{M_c n a^{9/4} (1-e)^{3/4} (1+e)^{11/4}} \sin\left(\frac{f}{2}\right) \left\{ -2 \cos\left(\frac{f}{2}\right) (2+e-\cos f) \left[\cos \omega (\cos \Omega + \sin \Omega) + \sin \omega (\sin i + \cos i (\cos \Omega - \sin \Omega)) \right] + 4 \sin^3\left(\frac{f}{2}\right) \left[\sin \omega (\cos \Omega + \sin \Omega) - \cos \omega (\sin i - \cos i (\sin \Omega - \cos \Omega)) \right] \right\}, \quad (22)$$

$$\frac{df}{dt} = \frac{n(1+e \cos f)^2}{(1-e^2)^{3/2}} - \frac{d\omega}{dt} - \cos i \frac{d\Omega}{dt}, \quad (23)$$

where i is the inclination, Ω is the longitude of ascending node, ω is the argument of pericentre and q is the pericentre distance. Note that the form of equation (23), without the subscript “sub”, is not restricted to sublimative forces.

Our main result can be hinted at directly by inspection from equations (17)-(23): for minor planets with orbital ec-

centricities near unity, sublimation-induced changes to the semimajor axis, eccentricity and pericentre distance are relatively strong, minor and negligible, respectively. Altering the pericentre distance of an orbit of a highly eccentric minor planet around a WD through sublimation alone is difficult. Other agents in the system are needed to perturb the minor planet into an orbit where it can tidally disrupt.

We can facilitate the coupling of GR with sublimation by considering the corresponding equations of motion in orbital elements. By assuming $M \ll M_{\text{WD}}$ to an excellent approximation we find (Veras 2014b)

$$\left(\frac{da}{dt}\right)_{\text{GR}} \approx \frac{2G^2 M_{\text{WD}}^2 e \sin f (1+e \cos f)^2}{c^2 n a^3 (1-e^2)^{7/2}} \times [7 + 3e^2 + 10e \cos f], \quad (24)$$

$$\left(\frac{de}{dt}\right)_{\text{GR}} \approx \frac{G^2 M_{\text{WD}}^2 \sin f (1+e \cos f)^2}{c^2 n a^4 (1-e^2)^{5/2}} \times [3 + 7e^2 + 10e \cos f], \quad (25)$$

$$\left(\frac{di}{dt}\right)_{\text{GR}} = \left(\frac{d\Omega}{dt}\right)_{\text{GR}} = 0, \quad (26)$$

$$\left(\frac{d\omega}{dt}\right)_{\text{GR}} \approx \frac{G^2 M_{\text{WD}}^2 (1+e \cos f)^2}{c^2 n a^4 e (1-e^2)^{5/2}} \times [(e^2 - 3) \cos f + 3e - 5e \cos(2f)], \quad (27)$$

$$\left(\frac{dq}{dt}\right)_{\text{GR}} = \frac{G^2 M_{\text{WD}}^2 \sin f (1+e \cos f)^2}{c^2 n a^3 (1-e)^{3/2} (1+e)^{7/2}} \times [-3 + 8e + e^2 - 10e \cos f]. \quad (28)$$

3.2 Planar orbital evolution equations

Equations (17)-(22) demonstrate how sublimation affects the entire set of orbital elements, including the inclination and longitude of ascending node. However, because WDs are extremely spherical compared to planets, the orbital architecture is rotationally symmetric. Hence, future WD studies might need to consider just the planar case. In order to obtain the equations for the planar case, we take the limit of zero inclination, and define the longitude of pericentre $\varpi = \Omega + \omega$.

For the planar equations of motion, the C variables which contain a subscript of “P” (below) are equivalent to those variables defined in equations (10)-(16) except that ω is replaced with ϖ . With these definitions, we can compactly express the coplanar equations of motion as

$$\left(\frac{da}{dt}\right)_{\text{sub}}^{\text{P}} = \frac{2D_0v_{g0}m_s r_0^{9/4} (1+e \cos f)^{9/4}}{M_c n a^{9/4} (1-e^2)^{11/4}} (C_{1\text{P}} - C_{2\text{P}}), \quad (29)$$

$$\left(\frac{de}{dt}\right)_{\text{sub}}^{\text{P}} = \frac{D_0v_{g0}m_s r_0^{9/4} (1+e \cos f)^{5/4}}{2M_c n a^{13/4} (1-e^2)^{7/4}} (C_{6\text{P}} - C_{5\text{P}}), \quad (30)$$

$$\left(\frac{d\varpi}{dt}\right)_{\text{sub}}^{\text{P}} = -\frac{D_0v_{g0}m_s r_0^{9/4} (1+e \cos f)^{5/4}}{2M_c n e a^{13/4} (1-e^2)^{7/4}} (C_{7\text{P}} + C_{9\text{P}}),$$

(31)

$$\left(\frac{dq}{dt}\right)_{\text{sub}}^{\text{P}} = -\frac{D_0 v_{\text{g0}} m_s r_0^{9/4} (1 + e \cos f)^{5/4}}{2 M_c n a^{9/4} (1 - e)^{3/4} (1 + e)^{11/4}} \times \left[\cos(2f + \varpi) + \cos \varpi (3 - 4 \cos f + 2e \sin f) - (3 - 2(2 + e) \sin f) \sin \varpi + 4 \sin(f + \varpi) - \sin(2f + \varpi) \right]. \quad (32)$$

Equations (29)-(32) show that even in the planar case, the orbital equations are still nontrivial functions of the true anomaly of the asteroid. Nevertheless, we can glean some physical insight from the formulae. The eccentricity terms in the denominator illustrate that $(da/dt)_{\text{sub}}$ will evolve more quickly than $(de/dt)_{\text{sub}}$, $(d\varpi/dt)_{\text{sub}}$, and $(dq/dt)_{\text{sub}}$.

For GR, because equations (24)-(25) and (27)-(28) are all independent of i , Ω and ω , we have

$$\left(\frac{da}{dt}\right)_{\text{GR}}^{\text{P}} = \left(\frac{da}{dt}\right)_{\text{GR}}, \quad (33)$$

$$\left(\frac{de}{dt}\right)_{\text{GR}}^{\text{P}} = \left(\frac{de}{dt}\right)_{\text{GR}}, \quad (34)$$

$$\left(\frac{dq}{dt}\right)_{\text{GR}}^{\text{P}} = \left(\frac{dq}{dt}\right)_{\text{GR}}, \quad (35)$$

$$\left(\frac{d\varpi}{dt}\right)_{\text{GR}}^{\text{P}} = \left(\frac{d\varpi}{dt}\right)_{\text{GR}}. \quad (36)$$

3.3 Numerical integrations

In this section we provide some specific examples of minor planet orbital evolution due to sublimation and GR.

3.3.1 Setup

First, we must establish some fiducial parameters. A crucial parameter is D_0 , which varies by several orders of magnitude in the Solar system. This variation should be even higher in WD systems because WD luminosities and spectral properties vary by orders of magnitude depending on the WD cooling age; WDs may be either more luminous or (much) less luminous than the Sun. Although the latter case holds in the majority of cases, D_0 cannot necessarily also be assumed to be lower because minor planets can reach much smaller values of q in WD systems. In fact, without being engulfed, a minor planet may attain $q = 6 \times 10^{-5}$ au. However, this value is well within the WD disruption radius, where the minor planet would likely be shorn apart. Instead, $q = 0.02$ au would nearly guarantee that the minor planet survives; actually survival is likely to be ensured over hundreds of orbits for values of q which are one or two orders of magnitude lower (Veras et al. 2014a). Complicating these considerations for determining a fiducial D_0 is that sublimation is a function of temperature and pressure, and significantly localized physical properties such as shadowing, thermal inhomogeneities, and spin.

Consequently, we defer linking D_0 with detailed internal minor planet models and WD cooling age to other studies. Instead, here we identify the value of D_0 in which

sublimative-induced orbital perturbations becomes significant for a minor planet which does not initially quite reach the WD disruption radius (for example, $q_0 = 0.02$ au). Like D_0 , the value of v_{g0} is intrinsically linked to local properties of the minor planet and is unknown outside of the Solar system. Fortunately, we can partially circumvent our ignorance by recognizing that all of the sublimation-based orbital evolution equations are directly proportional to the product $D_0 v_{\text{g0}}$. This property allows us to reduce the number of degrees of freedom in any phase space exploration. For our explorations, we choose the four products corresponding to the range $D_0 v_{\text{g0}} = (10^{26-29} \text{ mol/s}) \times (1 \text{ km/s})$. These speeds are easily achieved; in the Solar system, assuming a Maxwell-Boltzmann distribution, one obtains $\langle v_{\text{g0}} \rangle = 675 \pm 275 \text{ m/s}$ (with extreme speeds of several km/s) for temperatures of 360 K (Groussin et al. 2013).

Our other adopted values include $M_{\text{WD}} = 0.6 M_{\odot}$ (representing a typical WD; see Liebert et al. 2005; Camenzind 2007; Falcon et al. 2010; Tremblay et al. 2013), and $M_c = 10^{13} \text{ kg}$ (roughly corresponding to an active asteroid with a radius of 1 km and density of 2 g/cm^3). We place our minor planets on $a_0 = 10$ au orbits, because most km-sized minor planets within about 7 au will have been spun up to fission from giant branch radiation (Veras et al. 2014b). We do adopt $q = 0.02$ au, meaning that $e_0 = 0.998$, a typical eccentricity for a minor planet just missing the WD disruption radius. We sample minor planets on both slightly inclined ($\sim 1^\circ$; Figure 1) and highly inclined ($\sim 45^\circ$; Figure 2) orbits with respect to the same fixed but arbitrary reference plane. Our simulations begin at the pericentre and we propagate the systems for approximately 25 orbits. We integrate equations (17)-(21) and (23)-(27) all together.

3.3.2 Results

We present our results in Figs. 1-2. The sawtooth-like curves in both figures indicate that sublimation causes the greatest orbital changes at the pericentre, so that each step corresponds to one orbit.

Figure 1 showcases a side-by-side comparison when GR is not included (left panels) and is included (right panels) in the simulations. The difference is striking, particularly for the semimajor axis and pericentre evolution; for the blue, pink and green curves, at least, GR dominates over sublimation. Alternatively, the black curve for the evolution of ω indicates a regime where sublimation may dominate GR (after a few hundred yr). The figure makes clear that for reasonable parameters that one would expect in a WD system with planetary remnants, GR can play a crucial role and should be included in sublimation models.

Another comparison to consider in that figure is between the top and middle plots, whose y -axes are equivalent and in au. The change in $q - q_0$ is typically orders of magnitude less than the change in $a - a_0$, both with and without GR. GR dominates the evolution of q in most cases, flattening out the curves. In no case does q vary by more than 10^{-4} au.

In Figure 2, we include GR and show the time evolution for e , i , and Ω and as well as for a , q and ω , but now for minor planets with different initial values of i , Ω and ω . The highly inclined retrograde orbits sampled here yield different evolutions from Figure 1, but reinforce the main result: the

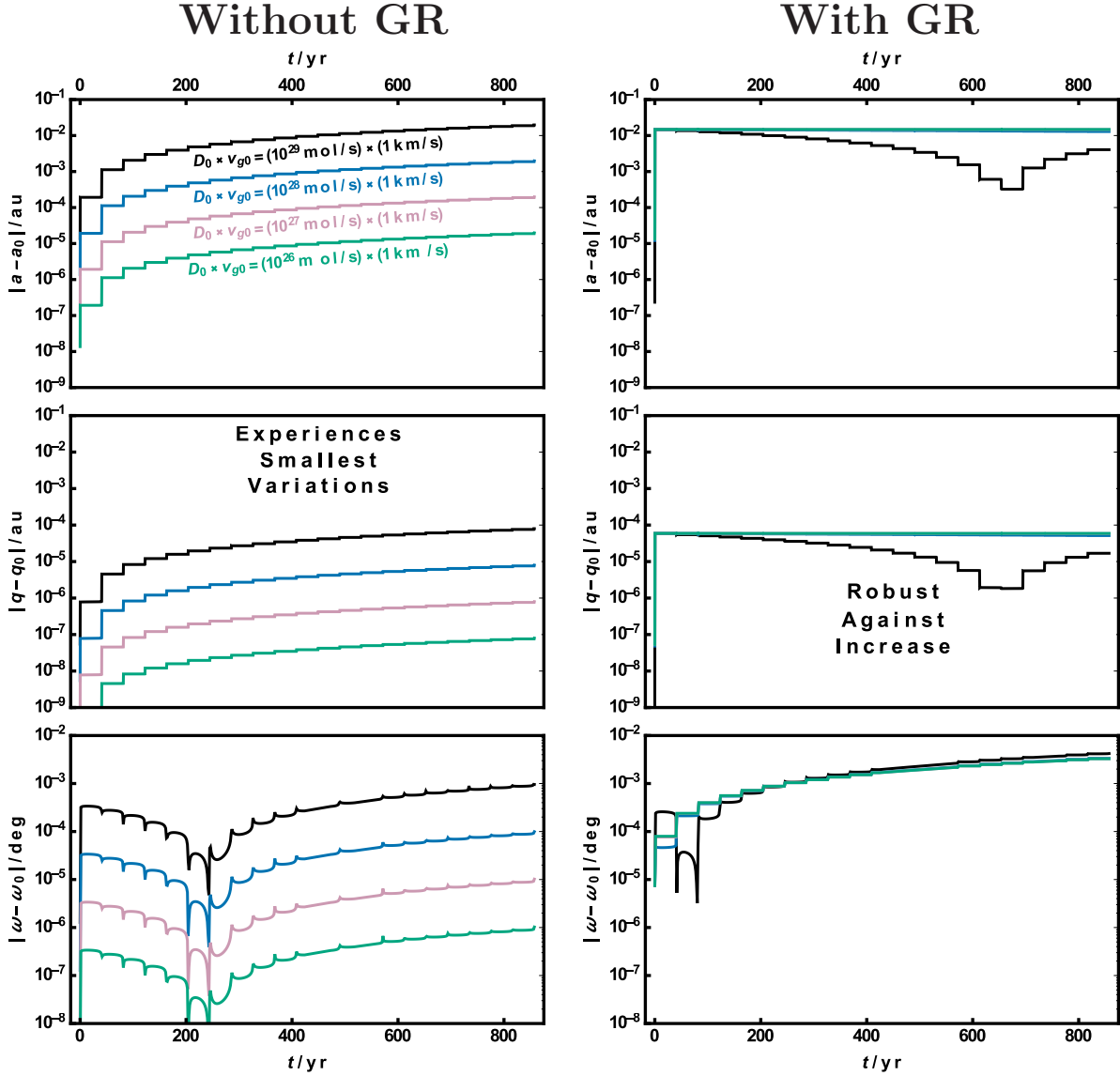


Figure 1. The orbital changes over about 25 orbits experienced by a 10^{13} kg minor planet orbiting a $0.6M_{\odot}$ star (like a WD) and sublimating water ice at a given rate D_0 and with a given speed v_{g0} . The product of D_0 and v_{g0} scales linearly with the change in each orbital element. The left panel does not include GR, and the right panel does. We set the initial minor planet orbit at $a_0 = 10$ au, $q_0 = 0.02$ au, $e_0 = 0.998$, $i_0 = 1.0^\circ$, $\Omega_0 = 180^\circ$, $\omega_0 = 1.0^\circ$ and $f_0 = 0.0^\circ$. The plot demonstrates the importance of including GR when the pericentre is close to the star, and hints that q cannot drift into the star’s disruption radius by the combined forces from sublimation and GR alone.

pericentre change does not exceed 2×10^{-4} au for any curve, whereas the semimajor axis may vary by as much as 0.05 au. Note that the two uppermost plots are drawn on the same scale.

For both sets of simulations, we also computed the total amount of mass actually lost by the minor planet from equation (7) throughout the evolution. This value is about 9.7×10^8 kg, four orders of magnitude less than than the core mass of the minor planet.

4 TRANSVERSE AND NONPLANAR OUTGASSING

So far our model for sublimation assumes that the nongravitational acceleration acts opposite to the radial direction. But what if the minor planet experiences a significant outgassing episode in another direction? In order to answer this question, we first consider a commonly-used formulation for outgassing in the Solar system.

4.1 Sublimation in the Solar system

This prescription effectively models a perturbed two-body problem, where the perturbative force is the product of a semiempirical functional form for water ice

With GR

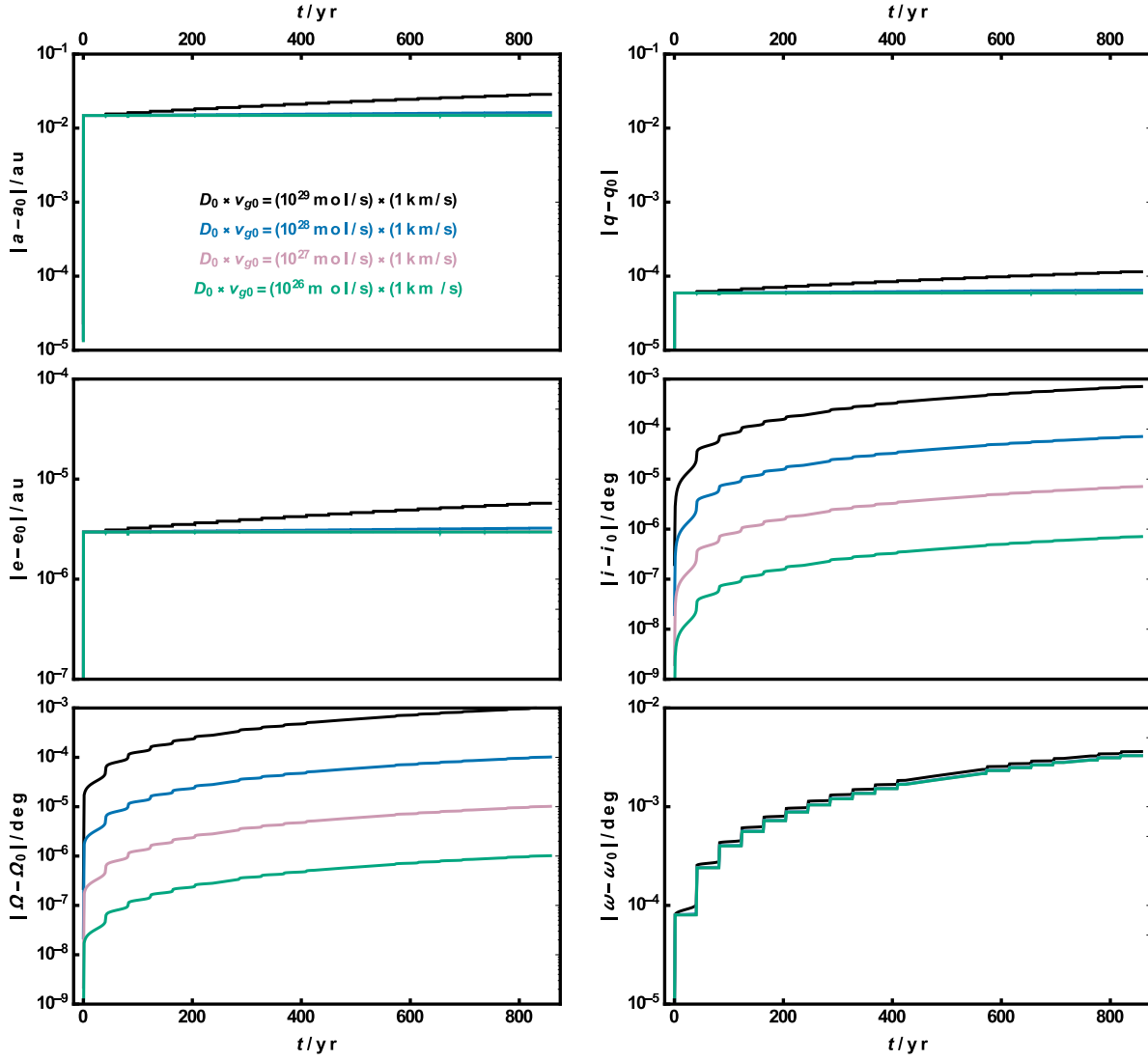


Figure 2. Like Figure 1, except with $i_0 = 45^\circ$, $\Omega_0 = 200^\circ$ and $\omega_0 = 135^\circ$. Both sublimation and GR are included in the simulation. Illustrated here are the time evolution of all of the orbital elements except f . Despite the minor planets having highly inclined orbits, q remains robust to major orbital changes.

(Delsemme & Miller 1971) and a linear combination of the radial, transverse and normal components of the motion (Marsden et al. 1973). Equation 1 of Sosa & Fernández (2011) and equation 1 of Szutowicz (2000) demonstrate that the Marsden formulation of outgassing for Solar system comets may be expressed as

$$\ddot{\vec{r}}_{\text{out}} = -\frac{G(M_\odot + M_c)}{r^3} + \mathbb{N}(r) \left[A_1 \underbrace{\frac{\vec{r}}{r}}_{\text{Radial} \equiv \hat{R}} + A_2 \underbrace{\frac{r\vec{v} - \vec{r}(\frac{\vec{r} \cdot \vec{v}}{r})}{|\vec{r} \times \vec{v}|}}_{\text{Transversal} \equiv \hat{T}} + A_3 \underbrace{\frac{\vec{r} \times \vec{v}}{|\vec{r} \times \vec{v}|}}_{\text{Normal} \equiv \hat{N}} \right], \quad (37)$$

$$\mathbb{N}(r) \equiv \alpha \left(\frac{r}{r_0} \right)^{-\eta} \left[1 + \left(\frac{r}{r_0} \right)^\xi \right]^{-\zeta} \quad (38)$$

such that the constants η , ξ and ζ are empirically derived, with typical fiducial values of 2.15, 5.093 and 4.6142, respectively. Further, the values of A_1 , A_2 and A_3 are not constant with time; for real comets, they can vary by an order of magnitude or more (see Table 2 of Froeschle & Rickman 1986 and Table 2 of Chesley & Yeomans 2005). Even this formulation, however, cannot explain many observational phenomena. For example, sometimes outgassing is not symmetric about the pericentre. Equation 5 of Królikowska (2004) takes into account such cases with related functional forms.

Note that we recover the formulation used in Section 3 by setting $A_2 = A_3 = 0$, $\eta = 9/4$, $\zeta = 0$ and $\alpha = \Theta(M_v) D_0 v_{g0} m_s / M_c$. We find the equation for the semi-major axis variation from the Marsden formulation to be

$$\left(\frac{da}{dt} \right)_{\text{out}} = \mathbb{N}(r) \times \frac{2[A_1 e \sin f + A_2(1 + e \cos f)]}{n(1 - e^2)^{1/2}}. \quad (39)$$

This form is equivalent to equation (24) of Burns (1976) (and equation (2.145) of Murray & Dermott 1999), but without the factor of $\mathbb{N}(r)$, even though we made no assumption about the magnitude of the nongravitational force (the force in those other studies is assumed to be small). The factor of $\mathbb{N}(r)$ does not alter the classical functional form obtained due to the radial, transverse and normal components. The evolution of the other orbital parameters are as follows and can also be re-expressed in the forms present in Burns (1976).

$$\left(\frac{de}{dt}\right)_{\text{out}} = \mathbb{N}(r) \times \frac{\sqrt{1-e^2}}{2na(1+e\cos f)} \times \left[2A_1 \sin f (1+e\cos f) + A_2 (4\cos f + e(3+\cos(2f))) \right], \quad (40)$$

$$\left(\frac{di}{dt}\right)_{\text{out}} = \mathbb{N}(r) \times A_3 \frac{\sqrt{1-e^2} \cos(f+\omega)}{an(1+e\cos f)}, \quad (41)$$

$$\left(\frac{d\Omega}{dt}\right)_{\text{out}} = \mathbb{N}(r) \times A_3 \frac{\sqrt{1-e^2} \csc i \sin(f+\omega)}{an(1+e\cos f)}, \quad (42)$$

$$\left(\frac{d\omega}{dt}\right)_{\text{out}} = -\mathbb{N}(r) \times \frac{\sqrt{1-e^2}}{na} \times \left[A_1 \frac{\cos f}{e} - A_2 \frac{\sin f(2+e\cos f)}{e(1+e\cos f)} + A_3 \frac{\cot i \sin(f+\omega)}{1+e\cos f} \right]. \quad (43)$$

From equations (39)-(40), we derive the change in pericentre q and apocentre Q as

$$\left(\frac{dq}{dt}\right)_{\text{out}} = \mathbb{N}(r) \times \frac{(1-e)^2}{2n\sqrt{1-e^2}(1+e\cos f)} \times \left[-2A_1 \sin f (1+e\cos f) + A_2 (4+e-4\cos f - e\cos(2f)) \right], \quad (44)$$

$$\left(\frac{dQ}{dt}\right)_{\text{out}} = \mathbb{N}(r) \times \frac{(1+e)^{3/2}}{2n\sqrt{1-e}(1+e\cos f)} \times \left[2A_1 \sin f (1+e\cos f) + A_2 (4-e+4\cos f + e\cos(2f)) \right]. \quad (45)$$

We see that $da/dt, de/dt, dq/dt$ and dQ/dt are unaffected by the choice of A_3 . If $A_3 = 0$ then the inclination and the longitude of the ascending node stay constant. If the motion is fully co-planar, i.e. $A_3 = 0$ and $i = 0$, then the ascending node is no longer well-defined and the evolution of the longitude of pericentre becomes

$$\left(\frac{d\varpi}{dt}\right)_{\text{out}}^{\text{P}} = \mathbb{N}(r) \times \frac{\sqrt{1-e^2}}{aen(1+e\cos f)} \times \left[-A_1 \cos f (1+e\cos f) + A_2 \sin f (2+e\cos f) \right]. \quad (46)$$

The formulae in this section allow one to model the evolution of a particular exosystem minor body for an assumed set of $\{A_1, A_2, A_3\}$. Currently, no such sets have been observationally measured outside of the Solar system.

4.2 Invariance of the pericentre

Regardless, we can reveal important properties of the motion by analyzing the equations alone. We know that orbital changes predominately occur during pericentre passages; consequently, we can expand the equations about $f = 0^\circ$. Further, in WD systems, any minor planets or comets which closely approach the WD must have extremely eccentric orbits ($e \geq 0.998$). Therefore, we can also Taylor expand the equations about $\epsilon = 1-e$, where $\epsilon \ll 1$. The following result shows the explicit dependencies on $(1-e)$, A_1 , A_2 and A_3 . We facilitate the expressions by first defining

$$\mathcal{N} \equiv \alpha \left(\frac{a(1-e)}{r_0} \right)^{-\eta} \left[1 + \left(\frac{a(1-e)}{r_0} \right)^\xi \right]^{-\zeta}. \quad (47)$$

We obtain

$$\left(\frac{da}{dt}\right)_{\text{out}} \Big|_{\substack{f \text{ about } 0^\circ \\ \epsilon \text{ about } 0}} = \mathcal{N} \left\{ -\frac{2\sqrt{2}}{n} (1-e)^{-\frac{1}{2}} A_2 + \mathcal{O} \left[(1-e)^{\frac{1}{2}} \right] \right\} + \mathcal{N} \left\{ -\frac{\sqrt{2}}{n} (1-e)^{-\frac{1}{2}} A_1 + \mathcal{O} \left[(1-e)^{\frac{1}{2}} \right] \right\} f + \mathcal{O} [f^2]. \quad (48)$$

Hence, the semimajor axis is most strongly influenced by a nonzero A_2 term, at the $(1-e)^{-1/2}$ order. The next strongest influence comes from a nonzero A_1 term at the $f(1-e)^{-1/2}$ order. The eccentricity dependencies are similar, except weaker by a factor of $(1-e)$:

$$\left(\frac{de}{dt}\right)_{\text{out}} \Big|_{\substack{f \text{ about } 0^\circ \\ \epsilon \text{ about } 0}} = \mathcal{N} \left\{ -\frac{2\sqrt{2}}{an} (1-e)^{\frac{1}{2}} A_2 + \mathcal{O} \left[(1-e)^{\frac{3}{2}} \right] \right\} + \mathcal{N} \left\{ -\frac{\sqrt{2}}{an} (1-e)^{\frac{1}{2}} A_1 + \mathcal{O} \left[(1-e)^{\frac{3}{2}} \right] \right\} f + \mathcal{O} [f^2]. \quad (49)$$

The inclination and longitude of ascending node terms are independent of A_1 and A_2 . Instead, these orbital parameters vary due to a nonzero A_3 , at the $(1-e)^{1/2}$ leading order as follows

$$\left(\frac{di}{dt}\right)_{\text{out}} \Big|_{\substack{f \text{ about } 0^\circ \\ \epsilon \text{ about } 0}} = \mathcal{N} \left\{ -\frac{\cos \omega}{\sqrt{2}an} (1-e)^{\frac{1}{2}} A_3 + \mathcal{O} \left[(1-e)^{\frac{3}{2}} \right] \right\} + \mathcal{N} \left\{ \frac{\sin \omega}{\sqrt{2}an} (1-e)^{\frac{1}{2}} A_3 + \mathcal{O} \left[(1-e)^{\frac{3}{2}} \right] \right\} f + \mathcal{O} [f^2], \quad (50)$$

$$\left(\frac{d\Omega}{dt}\right)_{\text{out}} \Big|_{\substack{f \text{ about } 0^\circ \\ \epsilon \text{ about } 0}} =$$

$$\begin{aligned} & \mathcal{N} \left\{ -\frac{\sin \omega}{\sqrt{2an \sin i}} (1-e)^{\frac{1}{2}} A_3 + \mathcal{O} \left[(1-e)^{\frac{3}{2}} \right] \right\} \\ & + \mathcal{N} \left\{ -\frac{\cos \omega}{\sqrt{2an \sin i}} (1-e)^{\frac{1}{2}} A_3 + \mathcal{O} \left[(1-e)^{\frac{3}{2}} \right] \right\} f + \mathcal{O} [f^2]. \end{aligned} \quad (51)$$

Unlike the evolution of a , e , i , and Ω , the evolution of ω is instead dominated by the combination of an A_1 term and a A_3 term, as follows

$$\begin{aligned} & \left(\frac{d\omega}{dt} \right)_{\text{out}} \Big|_{\substack{f \text{ about } 0^\circ \\ \epsilon \text{ about } 0}} = \\ & \mathcal{N} \left\{ \frac{2}{\sqrt{2an}} (1-e)^{\frac{1}{2}} A_1 + \frac{\cot i \sin \omega}{\sqrt{2an}} (1-e)^{\frac{1}{2}} A_3 \right. \\ & \quad \left. + \mathcal{O} \left[(1-e)^{\frac{3}{2}} \right] \right\} \\ & + \mathcal{N} \left\{ -\frac{3}{\sqrt{2an}} (1-e)^{\frac{1}{2}} A_2 + \frac{\cot i \cos \omega}{\sqrt{2an}} (1-e)^{\frac{1}{2}} A_3 \right. \\ & \quad \left. + \mathcal{O} \left[(1-e)^{\frac{3}{2}} \right] \right\} f + \mathcal{O} [f^2]. \end{aligned} \quad (52)$$

The coplanar version is

$$\begin{aligned} & \left(\frac{d\varpi}{dt} \right)_{\text{out}} \Big|_{\substack{f \text{ about } 0^\circ \\ \epsilon \text{ about } 0}} = \\ & \mathcal{N} \left\{ \frac{2}{\sqrt{2an}} (1-e)^{\frac{1}{2}} A_1 + \mathcal{O} \left[(1-e)^{\frac{3}{2}} \right] \right\} \\ & + \mathcal{N} \left\{ -\frac{3}{\sqrt{2an}} (1-e)^{\frac{1}{2}} A_2 + \mathcal{O} \left[(1-e)^{\frac{3}{2}} \right] \right\} f \\ & + \mathcal{O} [f^2]. \end{aligned} \quad (53)$$

Finally, now we compare the above results with the evolution of the pericentre

$$\begin{aligned} & \left(\frac{dq}{dt} \right)_{\text{out}} \Big|_{\substack{f \text{ about } 0^\circ \\ \epsilon \text{ about } 0}} = 0 \\ & + \mathcal{N} \left\{ \frac{1}{\sqrt{2n}} (1-e)^{\frac{3}{2}} A_1 + \mathcal{O} \left[(1-e)^{\frac{5}{2}} \right] \right\} f + \mathcal{O} [f^2]. \end{aligned} \quad (54)$$

Equation (54) demonstrates that (i) the pericentre undergoes no evolution at all in the leading order in true anomaly (f^0) term, (ii) in the next order term (f^1), the eccentricity dependence is weaker $[(1-e)^{3/2}]$ than that for any other orbital parameter, and (iii) this weaker leading-order term is independent of A_2 and A_3 , so that the best way to change the pericentre is through radial perturbations. The first two points illustrate how robust the orbital pericentre is to changes compared to any other orbital element.

5 DISCUSSION

Our conclusion is strong and independent of the detailed changes which a minor body or comet may experience after each pericentre passage if the lost volatiles do not constitute a large fraction of its total mass. In this case neither

outgassing nor sublimation can perturb a WD exosystem minor planet or comet into the WD disruption sphere if the original orbit remains outside of that sphere.

Although potential time dependencies of many of the parameters that we held constant, including D_0 and v_{go} , could certainly change a minor planet orbit, the actual pericentre cannot drift inward enough to transform an otherwise “safe” orbit into a “disruptable” one. Consequently, the presence of planets is necessary to perturb smaller bodies that reside within a few hundred au of the WD inside of the WD disruption sphere. In main sequence exosystems, the invariance of the pericentre distance also holds as long as the extrasolar minor planet or comet or is on a highly eccentric orbit. These systems do not necessarily need to host currently observable planets, as previous radial incursions from planet-planet scattering events can generate high eccentricities of smaller bodies that survive ejection (Veras & Armitage 2005, 2006; Raymond et al. 2010; Matsumura et al. 2013). Other potential sources of such high eccentricities are stellar flybys and Galactic tides; after a brief period of stellar mass loss, flybys and tides act in WD systems in a similar manner to main sequence planetary systems, including the Solar system (Veras et al. 2014d).

Because the timescales for orbital perturbations due to sublimation are short, and are often strongest at the first pericentre passage, they would likely dominate perturbations from WD radiation. Veras et al. (2015b) demonstrated that the ever-dimming WD radiation will shrink and circularize the orbits of sub-metre-sized particles eventually due to Poynting-Robertson drag. For the minor planets considered here, which are km-sized, the dominant radiative effect would be the Yarkovsky effect (Veras et al. 2015a). When activated, the Yarkovsky effect dominates Poynting-Robertson drag, but the timescale for Yarkovsky to act is still much longer than that from sublimation and GR. Consequently, for volatile-rich comets, sublimation likely alters the orbits before Yarkovsky becomes important. In these cases, sublimative forces in effect set the initial orbital conditions for other radiatively-induced perturbations. Alternatively, for volatile-depleted minor planets, only the relative strength of GR and the Yarkovsky effect would be important.

A sublimative perturbation on the semimajor axis of even just a few hundredths of an au may be significant. In WD systems that contain planets, that difference can break or initiate a mean motion resonance with a planet. Exo-Oort cloud comets which approach WDs (Alcock et al. 1986; Parriott & Alcock 1998; Veras et al. 2014c; Stone et al. 2015) may be ejected into the interstellar medium. In WD systems which are in the process of forming rings and discs from the tidal disruption of other minor planets, a change in semimajor axis will alter interactions with the resulting debris field during each pericentre passage. A significant debris field may already exist anyway from the end of the giant branch phases of evolution due to YORP break-up of km-sized asteroids, potentially extending to tens or hundreds of au (Veras et al. 2014b).

Finally, we note that the line between minor planets and comets may be fuzzy. Even in the Solar system, the distinction is not always easy to make (see, e.g., the Introduction of Jewitt et al. 2015). In fact, Weissman & Levison (1997) claimed that about 1 per cent of the Solar system Oort cloud

should comprise asteroids. Shannon et al. (2015) more recently suggested that this population of asteroids should be about eight billion.

6 CONCLUSIONS

Hard observational evidence of volatile-rich circumstellar material in WD systems motivates studies about how active asteroids and comets self-perturb their orbits due to the release of volatiles through sublimation and outgassing during close pericentre passages with the star. In this paper, we have derived the complete unaveraged equations of motion (17-23 and A2-A6) in orbital elements due only to sublimation, under some appropriate assumptions. These equations are widely applicable to general extrasolar systems assuming that planetary and external perturbations are negligible. For Solar-system-like sublimation rates, the effect of GR must be included (Fig. 1). We also considered the relative contribution of outgassing in the transverse and nonplanar directions, and presented corresponding equations (39-45) that also may be applied to exosystems.

These results, when applied to polluted WD systems, ultimately reveal that major planets must exist in order to perturb active asteroids into the WD disruption radius. Without major planets, these highly-eccentric minor planets cannot change their pericentre distances significantly enough through the release of volatiles. Inspection alone of equations (22), (28), (32) and (54) reveals why; the semimajor axis would change by many orders of magnitude more than the orbital pericentre in every case.

ACKNOWLEDGMENTS

We thank the referee for a probing and helpful report, and John H. Debes and Davide Farnocchia for useful discussions. The research leading to these results has received funding from the European Research Council under the European Union's Seventh Framework Programme (FP/2007-2013) / ERC Grant Agreement n. 320964 (WDTracer), EC Grant Agreement n. 282703 (NEOShield) and EC Grant Agreement n. 640351 (NEOShield-2) as well as Paris Observatory's ESTERS (Environnement Spatial de la Terre : Recherche & Surveillance) travel grants.

Table A1. Powers of $(1 - e)$ in the leading order term for the stated expressions expanded about high eccentricity. For $W \geq 2$, the pericentre distance is more resistant to change than any other variable.

W	$\left\langle \left(\frac{da}{dt} \right)_{\text{sub}}^{\text{P}} \right\rangle$	$\left\langle \left(\frac{de}{dt} \right)_{\text{sub}}^{\text{P}} \right\rangle$	$\left\langle \left(\frac{dq}{dt} \right)_{\text{sub}}^{\text{P}} \right\rangle$	$\left\langle \left(\frac{d\varpi}{dt} \right)_{\text{sub}}^{\text{P}} \right\rangle$
1	0	1/2	1/2	1/2
2	-1	0	1/2	0
3	-2	-1	0	-1
4	-3	-2	-1	-2
5	-4	-3	-2	-3
6	-5	-4	-3	-4
7	-6	-5	-4	-5

APPENDIX A: SUBLIMATION WITH DIFFERENT POWER LAWS

In order to assess how strongly dependent our sublimation findings are on the specific power-law prescription used in equation (6), we now rederive the equations of motion under more general considerations. Our physical motivation for the power-law exponent was observations from within the Solar system. However, to allow for unknown variations that can arise in the populations of small bodies in exosystems, we assume the equation of motion for a sublimating small body is instead given by

$$\ddot{r}_{\text{sub}} \approx -\frac{G(M_{\text{WD}} + M_c) \bar{r}}{r^3} - \frac{\alpha}{M_c} \left(\frac{r_0}{r} \right)^W \frac{\bar{r}}{r} \quad (\text{A1})$$

where W is a positive integer and α is a constant. This integer requirement will allow us to obtain averaged quantities analytically, and further bound the observationally-motivated value with $W = 2$ and $W = 3$. This exercise will allow one to easily derive the equations of motion for an arbitrary power-law perturbation to the two-body problem algebraically.

We find that the terms containing the i , Ω and the C variables remain unchanged such that

$$\left(\frac{da}{dt} \right)_{\text{sub}} = \frac{2\alpha r_0^W (1 + e \cos f)^W}{M_c n a^W (1 - e^2)^{W + \frac{1}{2}}} \left[C_1 (\cos i \cos \Omega - \cos i \sin \Omega + \sin i) - C_2 (\cos \Omega + \sin \Omega) \right] \quad (\text{A2})$$

$$\left(\frac{de}{dt} \right)_{\text{sub}} = \frac{\alpha r_0^W (1 + e \cos f)^{W-1}}{2M_c n a^{W+1} (1 - e^2)^{W - \frac{1}{2}}} \left[C_6 (\cos i \cos \Omega - \cos i \sin \Omega + \sin i) - C_5 (\cos \Omega + \sin \Omega) \right], \quad (\text{A3})$$

$$\left(\frac{di}{dt} \right)_{\text{sub}} = \frac{\alpha r_0^W (1 + e \cos f)^{W-1} \cos(f + \omega)}{M_c n a^{W+1} (1 - e^2)^{W - \frac{1}{2}}} \sin i (\sin \Omega - \cos \Omega + \cot i), \quad (\text{A4})$$

$$\left(\frac{d\Omega}{dt} \right)_{\text{sub}} = \frac{\alpha r_0^W (1 + e \cos f)^{W-1} \sin(f + \omega)}{M_c n a^{W+1} (1 - e^2)^{W - \frac{1}{2}}} (\sin \Omega - \cos \Omega + \cot i), \quad (\text{A5})$$

$$\left(\frac{d\omega}{dt} \right)_{\text{sub}} = \frac{-\alpha r_0^W (1 + e \cos f)^{W-1}}{2M_c n e a^{W + \frac{1}{2}} (1 - e^2)^W} \left[C_8 (\cos i \cos \Omega - \cos i \sin \Omega) + C_9 \sin i + C_7 (\cos \Omega + \sin \Omega) + 2e \sin(f + \omega) \cos i \cot i \right], \quad (\text{A6})$$

$$\left(\frac{da}{dt} \right)_{\text{sub}}^{\text{P}} = \frac{2\alpha r_0^W (1 + e \cos f)^W}{M_c n a^W (1 - e^2)^{W + \frac{1}{2}}} (C_{1\text{P}} - C_{2\text{P}}), \quad (\text{A7})$$

$$\left(\frac{de}{dt} \right)_{\text{sub}}^{\text{P}} = \frac{\alpha r_0^W (1 + e \cos f)^{W-1}}{2M_c n a^{W+1} (1 - e^2)^{W - \frac{1}{2}}} (C_{6\text{P}} - C_{5\text{P}}), \quad (\text{A8})$$

$$\left(\frac{d\varpi}{dt} \right)_{\text{sub}}^{\text{P}} = -\frac{\alpha r_0^W (1 + e \cos f)^{W-1}}{2M_c n e a^{W + \frac{1}{2}} (1 - e^2)^{W - \frac{1}{2}}} (C_{7\text{P}} + C_{9\text{P}}), \quad (\text{A9})$$

Averaging the above equations presents difficulties analytically and would typically require the use of computer algebra software. Even with that tool, we could obtain only the averaged planar equations of motion. We accomplish this task as in Veras (2014a) by computing integrals symbolically where the integrand is a function of an integral power of $(1 + e \cos f)$ multiplied by single powers of $\sin(kf)$ and $\cos(kf)$, where k is an integer greater than or equal to 1.

The resulting expressions, denoted by $\langle \rangle$, are long and we do not present them. Instead, we expand the expressions in a Taylor series about $\epsilon = 1 - e$, $\epsilon \ll 1$, and consider the leading term in the expansion (denoted by a wide tilde). We hence report the lowest-order power of $(1 - e)$ appearing in this expansion in Table A1.

Because this power is higher for the pericentre distance than for the evolution of any other variable for $W \geq 2$, we conclude that our main finding is robust for a wide variety of steeper potential sublimation power-law profiles.

REFERENCES

- A'Hearn, M. F., Millis, R. C., Schleicher, D. O., Osip, D. J., & Birch, P. V. 1995, *Icarus*, 118, 223
- Aannestad, P. A., Kenyon, S. J., Hammond, G. L., & Sion, E. M. 1993, *AJ*, 105, 1033
- Adams, F. C., Anderson, K. R., & Bloch, A. M. 2013, *MNRAS*, 432, 438
- Alcock, C., Fristrom, C. C., & Siegelman, R. 1986, *ApJ*, 302, 462
- Bear, E., & Soker, N. 2013, *New Astronomy*, 19, 56
- Becklin, E. E., Farihi, J., Jura, M., et al. 2005, *ApJL*, 632, L119
- Bergfors, C., Farihi, J., Dufour, P., & Rocchetto, M. 2014, *MNRAS*, 444, 2147
- Beutler, G. 2005, *Methods of celestial mechanics*. Vol. I / Gerhard Beutler. In cooperation with Leos Mervart and Andreas Verdun. *Astronomy and Astrophysics Library*. Berlin: Springer, ISBN 3-540-40749-9, 2005, XVI, 464 pp.
- Bonsor, A., & Wyatt, M. 2010, *MNRAS*, 409, 1631
- Bonsor, A., Mustill, A. J., & Wyatt, M. C. 2011, *MNRAS*, 414, 930
- Brown, J. C., Potts, H. E., Porter, L. J., & Le Chat, G. 2011, *A&A*, 535, A71
- Burns, J. A. 1976, *American Journal of Physics*, 44, 944
- Camenzind, M., *Astronomy and Astrophysics Library, Compact Objects in Astrophysics: White Dwarfs, Neutron Stars and Black Holes*. Springer-Verlag, Berlin.
- Chesley, S. R., & Yeomans, D. K. 2005, *IAU Colloq. 197: Dynamics of Populations of Planetary Systems*, 289
- Debes, J. H., & Sigurdsson, S. 2002, *ApJ*, 572, 556
- Debes, J. H., Walsh, K. J., & Stark, C. 2012, *ApJ*, 747, 148
- Delsemme, A. H., & Miller, D. C. 1971, *Planetary and Space Science*, 19, 1229
- Dong, R., Wang, Y., Lin, D. N. C., & Liu, X.-W. 2010, *ApJ*, 715, 1036
- Efroimsky, M. 2005, *Annals of the New York Academy of Sciences*, 1065, 346
- Falcon, R. E., Winget, D. E., Montgomery, M. H., & Williams, K. A. 2010, *ApJ*, 712, 585
- Farihi, J., Jura, M., & Zuckerman, B. 2009, *ApJ*, 694, 805
- Farihi, J., Barstow, M. A., Redfield, S., Dufour, P., & Hambly, N. C. 2010, *MNRAS*, 404, 2123
- Farihi, J., Gänsicke, B. T., Steele, P. R., et al. 2012, *MNRAS*, 421, 1635
- Farihi, J., Gänsicke, B. T., & Koester, D. 2013, *Science*, 342, 218
- Festou, M. C., Rickman, H., & West, R. M. 1993, *Astronomy & Astrophysics Review*, 5, 37
- Fouchard, M., Froeschlé, C., Valsecchi, G., & Rickman, H. 2006, *Celestial Mechanics and Dynamical Astronomy*, 95, 299
- Frewen, S. F. N., & Hansen, B. M. S. 2014, *MNRAS*, 439, 2442
- Fregeau, J. M., Cheung, P., Portegies Zwart, S. F., & Rasio, F. A. 2004, *MNRAS*, 352, 1
- Friedrich, S., Jordan, S., & Koester, D. 2004, *A&A*, 424, 665
- Froeschle, C., & Rickman, H. 1986, *A&A*, 170, 145
- Gänsicke, B. T., Marsh, T. R., Southworth, J., & Rebassa-Mansergas, A. 2006, *Science*, 314, 1908
- Gänsicke, B. T., Marsh, T. R., & Southworth, J. 2007, *MNRAS*, 380, L35
- Gänsicke, B. T., Koester, D., Marsh, T. R., Rebassa-Mansergas, A., & Southworth, J. 2008, *MNRAS*, 391, L103
- Gänsicke, B. T. 2011, *American Institute of Physics Conference Series*, 1331, 211
- Graham, J. R., Matthews, K., Neugebauer, G., & Soifer, B. T. 1990, *ApJ*, 357, 216
- Groussin, O., Sunshine, J. M., Feaga, L. M., et al. 2013, *Icarus*, 222, 580
- Gurfil, P. 2007, *Acta Astronautica*, 60, 71
- Hadjidemetriou J. D., 1963, *Icarus*, 2, 440
- Hansen, C. J., Esposito, L., Stewart, A. I. F., et al. 2006, *Science*, 311, 1422
- Heisler, J., & Tremaine, S. 1986, *Icarus*, 65, 13
- Holberg, J. B., Oswald, T. D., & Barstow, M. A. 2012, *AJ*, 143, 68
- Jewitt, D., Agarwal, J., Weaver, H., Mutchler, M., & Larson, S. 2013, *ApJL*, 778, L21
- Jewitt, D., Hsieh, H., & Agarwal, J. 2015, arXiv:1502.02361, In Press, *Asteroids IV book*, Eds. P. Michel, F. DeMeo and W. Bottke.
- Jura, M. 2003, *ApJL*, 584, L91
- Jura, M. 2006, *ApJ*, 653, 613
- Jura, M., & Xu, S. 2010, *AJ*, 140, 1129
- Jura, M., & Xu, S. 2012, *AJ*, 143, 6
- Kilic, M., von Hippel, T., Leggett, S. K., & Winget, D. E. 2005, *ApJL*, 632, L115
- Kilic, M., & Redfield, S. 2007, *ApJ*, 660, 641
- Knight, M. M., & Battams, K. 2014, *ApJL*, 782, LL37
- Koester, D., Gänsicke, B. T., & Farihi, J. 2014, *A&A*, 566, A34
- Korsun, P. P., Kulyk, I. V., Ivanova, O. V., et al. 2010, *Icarus*, 210, 916
- Korsun, P. P., Rousselot, P., Kulyk, I. V., Afanasiev, V. L., & Ivanova, O. V. 2014, *Icarus*, 232, 88
- Kratter, K. M., & Perets, H. B. 2012, *ApJ*, 753, 91
- Królikowska, M. 2004, *A&A*, 427, 1117
- Liebert, J., Bergeron, P., & Holberg, J. B. 2005, *ApJS*, 156, 47
- Luhman, K. L., Burgasser, A. J., & Bochanski, J. J. 2011, *ApJL*, 730, LL9
- Maquet, L., Colas, F., Jorda, L., & Crovisier, J. 2012, *A&A*, 548, A81
- Maquet, L. 2015, In Press, *A&A*, arXiv:1412.1983
- Manser, C., et al. In Preparation *MNRAS*
- Marsden, B. G., Sekanina, Z., & Yeomans, D. K. 1973, *AJ*, 78, 211
- Marsh, T. R., Parsons, S. G., Bours, M. C. P., et al. 2014, *MNRAS*, 437, 475
- Matsumura, S., Ida, S., & Nagasawa, M. 2013, *ApJ*, 767, 129
- Melis, C., Dufour, P., Farihi, J., et al. 2012, *ApJL*, 751, L4
- Mottola, S., Lowry, S., Snodgrass, C., et al. 2014, *A&A*, 569, LL2
- Murray, C. D., & Dermott, S. F. 1999, *Solar system dynamics by Murray, C. D., 1999*,
- Mustill, A. J., Veras, D., & Villaver, E. 2014, *MNRAS*, 437, 1404
- Parriott, J., & Alcock, C. 1998, *ApJ*, 501, 357
- Pierret, F. 2014, arXiv:1402.1758

- Omarov T. B., 1962, *Izv. Astrofiz. Inst. Acad. Nauk. KazSSR*, 14, 66
- Raddi, R., Gänsicke, B. T., Koester, D., et al. 2015, *MNRAS*, 450, 2083
- Raymond, S. N., Armitage, P. J., & Gorelick, N. 2010, *ApJ*, 711, 772
- Reach, W. T., Kuchner, M. J., von Hippel, T., et al. 2005, *ApJL*, 635, L161
- Rickman, H., & Froeschlé, C. 1987, *Celestial Mechanics*, 43, 243
- Rocchetto, M., Farihi, J., Gänsicke, B. T., & Bergfors, C. 2015, *MNRAS*, 449, 574
- Sanzovo, G. C., de Almeida, A. A., Misra, A., et al. 2001, *MNRAS*, 326, 852
- Shannon, A., Jackson, A. P., Veras, D., & Wyatt, M. 2015, *MNRAS*, 446, 2059
- Sosa, A., & Fernández, J. A. 2009, *MNRAS*, 393, 192
- Sosa, A., & Fernández, J. A. 2011, *MNRAS*, 416, 767
- Stone, N., Metzger, B. D., & Loeb, A. 2015, *MNRAS*, 448, 188
- Szutowicz, S. 2000, *A&A*, 363, 323
- Szutowicz, S., & Rickman, H. 2006, *Icarus*, 185, 223
- Tremblay, P. E., Ludwig, H. G., Steffen, M., & Freytag, B. 2013, *A&A*, 559, 104
- Veras, D., & Armitage, P. J. 2005, *ApJL*, 620, L111
- Veras, D., & Armitage, P. J. 2006, *ApJ*, 645, 1509
- Veras, D., Wyatt, M. C., Mustill, A. J., Bonsor, A., & Eldridge, J. J. 2011, *MNRAS*, 417, 2104
- Veras, D., & Moeckel, N. 2012, *MNRAS*, 425, 680
- Veras, D., & Tout, C. A. 2012, *MNRAS*, 422, 1648
- Veras, D., Hadjidemetriou, J. D., & Tout, C. A. 2013a, *MNRAS*, 435, 2416
- Veras, D., Mustill, A. J., Bonsor, A., & Wyatt, M. C. 2013b, *MNRAS*, 431, 1686
- Veras, D., & Evans, N. W. 2013a, *Celestial Mechanics and Dynamical Astronomy*, 115, 123
- Veras, D., & Evans, N. W. 2013b, *MNRAS*, 430, 403
- Veras, D. 2014a, *Celestial Mechanics and Dynamical Astronomy*, 118, 315
- Veras, D. 2014b, *MNRAS*, 442, L71
- Veras, D., Leinhardt, N. W., Bonsor, A., Gänsicke, B. T. 2014a, *MNRAS*, 445, 2244
- Veras, D., Jacobson, S. A., Gänsicke, B. T. 2014b, *MNRAS*, 445, 2794
- Veras, D., Shannon, A., Gänsicke, B. T. 2014c, *MNRAS*, 445, 4175
- Veras, D., Evans, N. W., Wyatt, M. C., & Tout, C. A. 2014d, *MNRAS*, 437, 1127
- Veras, D., Gänsicke, B. T. 2015, *MNRAS*, 447, 1049
- Veras, D., Eggl, S., Gänsicke, B. T., 2015a, In Press, *MNRAS*, arXiv:1505.01851
- Veras, D., Leinhardt, Z.M., Eggl, S., Gänsicke, B. T., 2015b, In Press, *MNRAS*, arXiv:1505.06204
- Voyatzis, G., Hadjidemetriou, J. D., Veras, D., & Varvoglis, H. 2013, *MNRAS*, 430, 3383
- Weissman, P. R., & Levison, H. F. 1997, *ApJL*, 488, L133
- Whipple, F. L. 1950, *ApJ*, 111, 375
- Wilson, D. J., Gänsicke, B. T., Koester, D., et al. 2014, *MNRAS*, 445, 1878
- Wilson, D. J., Gänsicke, B. T., Koester, D., et al. 2015, In Press *MNRAS*, arXiv:1505.07466
- Wyatt, M. C., Farihi, J., Pringle, J. E., & Bonsor, A. 2014, *MNRAS*, 439, 3371
- Yeomans, D. K., Yau, K. K., & Weissman, P. R. 1996, *Icarus*, 124, 407
- Zakamska, N. L., & Tremaine, S. 2004, *AJ*, 128, 869
- Zuckerman, B., & Becklin, E. E. 1987, *Nature*, 330, 138
- Zuckerman, B., Koester, D., Reid, I. N., Hüensch, M. 2003, *ApJ*, 596, 477
- Zuckerman, B., Melis, C., Klein, B., Koester, D., & Jura, M. 2010, *ApJ*, 722, 725